

Journal of
Applied Remote Sensing

**Comparison of sea-level measurements
between microwave radar and
subsurface pressure gauge deployed at
select locations along the coast of India**

Prakash Mehra
Ramachandra Gopal Prabhudesai
Antony Joseph
Vijay Kumar
Yogesh Agarvadekar
Ryan Luis
Lalsab Nadaf

Comparison of sea-level measurements between microwave radar and subsurface pressure gauge deployed at select locations along the coast of India

Prakash Mehra, Ramachandra Gopal Prabhudesai, Antony Joseph, Vijay Kumar, Yogesh Agarvadekar, Ryan Luis, and Lalsab Nadaf

Council of Scientific and Industrial Research–National Institute of Oceanography,
Dona Paula-403004, Goa, India
pmehra@nio.org

Abstract. Sea-level data are obtained from several remote and coastal locations using absolute pressure gauges deployed at known level, known as chart datum. However, to yield correct sea-level measurements from absolute pressure measurements, it is necessary to take into account the atmospheric pressure and water density at the measurement locations. We used data collected from microwave radar and an absolute pressure gauge deployed at Verem, Goa (January 2009 to May 2010), Tuticorin, and Mandapam, Tamil Nadu (June 2010 to March 2011) to carry out comparative studies. The root-mean-square difference between the estimated sea level from radar and pressure gauge (incorporating atmospheric pressure correction) is ~2.69, 2.73, and 1.46 cm at Verem, Tuticorin, and Mandapam, respectively. Harmonic analysis of the two time-series of sea-level data at Verem produces similar residuals and tidal constituents. Our results indicate the importance of concurrent measurement of atmospheric pressure along with subsurface absolute pressure gauge measurements. Internet-based real-/near-real-time tracking and monitoring of sea level, sea state, and surface-meteorological conditions from a network of several island and coastal stations provides considerable information to disaster managers and local administrators during episodic events such as storms, storm surges, and tsunamis. © The Authors. Published by SPIE under a Creative Commons Attribution 3.0 Unported License. Distribution or reproduction of this work in whole or in part requires full attribution of the original publication, including its DOI. [DOI: [10.1117/1.JRS.7.073569](https://doi.org/10.1117/1.JRS.7.073569)]

Keywords: sea level; radar and pressure gauges; comparison; variability; internet accessibility; real-time reporting; ocean and coastal management.

Paper 12212P received Jul. 20, 2012; revised manuscript received Mar. 12, 2013; accepted for publication Mar. 13, 2013; published online May 3, 2013.

1 Introduction

Information on sea level and its variability along coastal locations is essential for operational applications as well as scientific studies. Apart from safer navigational and coastal management activities at local level, sea-level data are also needed for measuring and predicting storm surges, understating the current sea-level variability and its implications to the coastal population (e.g., Refs. 1 and 2), validating circulation models and calibrating satellite radar altimeters (e.g., Refs. 3–5). On a global scale, sea-level studies are crucial to understand the changes in the Earth's climate and its multidecadal fluctuations (e.g., Refs. 6–8). The average global sea-level rise, which is consistent with warming, is estimated at an average rate of 1.8 (1.3 to 2.3) mm per year over the period of 1963 to 2003.⁹ However, the disastrous consequences of the recent Japan tsunami (March 11, 2011), impact of the powerful December 2004 global tsunami,^{10,11} and the historically known vulnerability of the Indian coasts to storm surges¹² emphasize the need for real-/near-real-time reporting of sea level, sea state, and surface meteorological information for multihazard monitoring and warning purposes. Although a single system at a given location may not be of much practical use for warning, a network of spatially distributed real-/near-real-time reporting gauges in the coastal and island locations will be greatly beneficial to disaster managers and local administrators because a signal of any natural event

takes time to travel from the source region to a distant location. In such a situation, a network of real-/near-real-time reporting gauges will allow monitoring of the progress of the event, helping the decision-makers to take necessary precautions.

The December 2004 Indian Ocean tsunami episode prompted all countries with ocean boundaries to prepare for a possible disaster due to tsunamis and storm surges. Since then, many countries have developed and deployed deep-ocean tsunami monitoring systems and networks of real-time monitoring coastal sea-level gauges; other countries are in the process of establishing such systems. It is prudent for countries with coastlines vulnerable to tsunamis and storm surges to have prior knowledge of technologies that are suitable for their specific needs. As many of the countries that are threatened by tsunamis are resource-limited, choosing the wrong or inappropriate technology may lead to heavy casualties during the next episode. A comprehensive description that offers an unbiased comparative evaluation and assessment of the optimum technology suitable for specific situations is given by Joseph,¹³ Martin et al.,^{14,15} Kranz et al.,¹⁶ and Woodworth and Smith¹⁷ reported the test results of radar tide gauges manufactured by different firms and comparison between other types of gauges. Thus, relative performance of different systems and evaluation of technologies serve as a reference to the personnel responsible for protecting the coastal population.

In this paper, we report the experience gained in developing and operating an Integrated Coastal Observation Network (ICON), which is Internet accessible and provides cellular-based real-/near-real-time sea level, sea state, and surface meteorological observations, established by the Council of Scientific and Industrial Research–National Institute of Oceanography (CSIR-NIO), Goa, India, at several locations on the Indian coasts and islands [Fig. 1(a); <http://inet.nio.org>]. The first real-/near-real-time reporting cellular-based sea-level station was established in Verem, Goa, in September 2005. The present study is aimed at comparing the sea-level measurements from the downward-looking aerial microwave radar and pressure gauge and evaluating the importance of atmospheric pressure variability in estimating the sea level using subsurface absolute pressure gauges at Verem in Goa and Tuticorin and Mandapam in Tamil Nadu, India. In Sec. 2, we briefly address the theory of pressure and radar gauge (RG) systems, and in Sec. 3, we briefly describe the means and methods for comparative analysis; the results of analysis are presented in Sec. 4.

2 Sea-Level Measurement Methods

The most common sea-level measuring technologies are stilling-well and float, pressure system, acoustic system, and radar system.¹⁸ In this section, we briefly describe the principle of operation of pressure and RG systems.

2.1 Pressure Gauge

These systems measure the subsurface pressure [Fig. 2(a)] according to the following law:

$$h = \frac{(p - p_a)}{\rho \times g}, \quad (1)$$

where h is the height of the instantaneous sea surface above the pressure port, p is the measured subsurface pressure, p_a is the atmospheric pressure, ρ is the water density, and g is Earth's gravitational acceleration. Therefore, this system requires knowledge of local atmospheric pressure, water density, and local gravity. The density ρ is important in estuarine waters, as it undergoes seasonal variability due to changes in fresh water influx as well as semi-diurnal variability of tidal cyclicity. In such cases, density corrections need to be incorporated during postprocessing. However, in locations where the water is well mixed, density can be considered constant. The pressure gauge at Verem jetty uses pressure sensor from Honeywell Inc. (Table 1) and is deployed ~ 1 m below the chart datum (CD) with its electronics, power supply, and solar panel at the top of the mounting structure fixed to the jetty as shown in Fig. 2(a). The

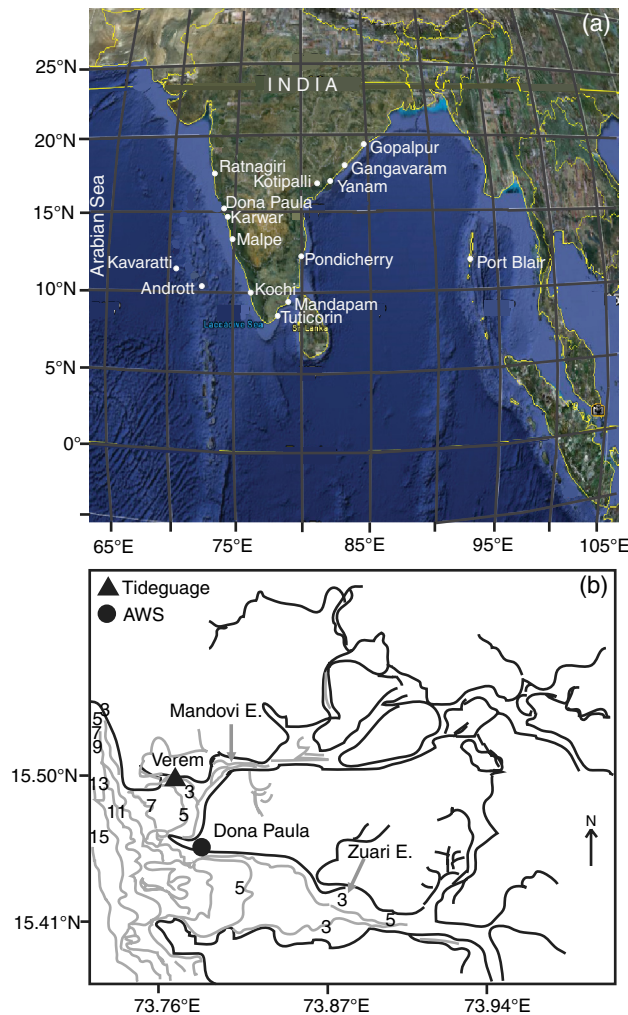


Fig. 1 Maps showing (a) the network of near-real-time reporting sea level and surface meteorological systems along the islands and coast of India, and (b) the study region, Verem, Goa, India.

self-recording-type pressure gauges from Sea-Bird Electronics Inc. with metallic housing were deployed near the RGs, resting on the sea bed (depth ~ 2 m) at Tuticorin and Mandapam. The metallic housing of the pressure gauge acted as dead weight (~ 50 kg) to minimize the drift of the gauges; it was anchored with chains to the nearby jetty.

2.2 Radar Gauge

The radar sensor is positioned [Fig. 2(b)] well above the highest expected sea level (also the highest expected wave to avoid damages to the unit) and measures the aerial distance from the sensor to the water surface. Radar is a noncontact device that is capable of remote measurement of sea-level elevation from the air. The transmission frequency of the radar sensor is ~ 24 GHz and the beam width is $\sim \pm 5$ deg. The basic premise involved in the operation of the radar sensor is transmission of microwave pulses toward the sea surface and reception of the reflected/backscattered energy. The reflected microwaves are analyzed to estimate the aerial distance traveled by a given pulse. Averaging over 30 s filters out short-period variability due to wind-waves and swells. Sea-level elevation (H), referenced to CD, is obtained by subtracting the measured aerial distance (L) from the height (K), of the radar sensor above CD. The RG has many advantages over the traditional systems,¹⁸ as it makes direct measurements of sea level. The effect of density and temperature variations, even in the atmosphere, are unimportant. On

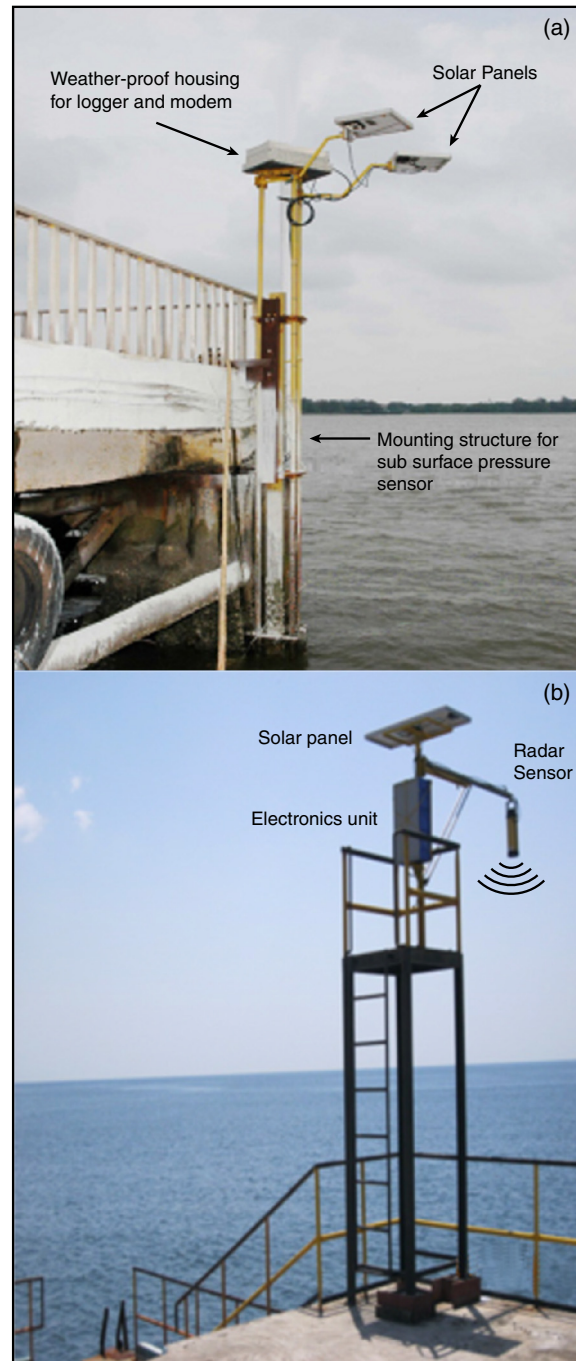


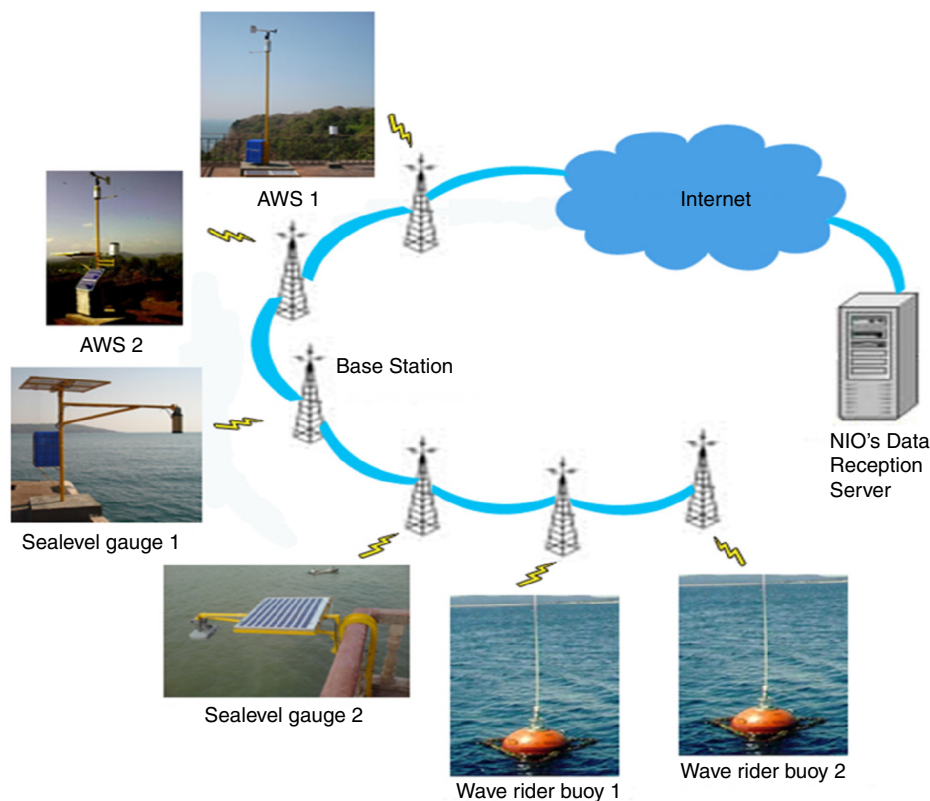
Fig. 2 Typical installations of (a) subsurface pressure gauge (PG) and (b) downward-looking aerial microwave radar gauge (RG).

account of these superior qualities, the RG is used as a reference system in the present comparative study.

The typical configuration of subsurface pressure sensors and downward-looking microwave radars incorporated in the ICON are shown in Fig. 3. The sea-level information acquired using dedicated Linux-based data loggers and uploaded to an Internet server using GPRS cellular modems are available in graphical format at <http://inet.nio.org>. The radar-level sensor from OTT Hydromet GmbH (OTT-RLS) is used in the RGs of ICON in order to meet the national and international needs of sea-level monitoring and compatibility to the Global Sea Level Observation (GLOSS) program. They feature the common characteristics listed in Table 1.

Table 1 Major technical specifications of the sensors used in radar gauges (RGs) and pressure gauges (PGs) deployed at Verem, Goa, and SBE26 deployed at Tuticorin and Mandapam, Tamil Nadu.

S. N.	Specifications	Radar gauge sensor	Pressure gauge sensor
1	Make	OTT Hydromet GmbH Radar-level sensor (OTT-RLS)	Honeywell Inc. Precision pressure transducer-ruggedized (PPTR) Seagauge SBE26plus Sea-Bird Electronics
2	Range (m)	2 to 30	0 to 18 0 to 20
3	Accuracy (mm)	± 3	± 18 ± 3
4	Resolution (mm)	1	0.2 0.01
5	Integration time (min)	5	5 1

**Fig. 3** Schematic of the network of distributed real-time reporting sea level, sea state, and surface meteorological MET stations.

3 Data and Method

In this section, we provide a brief description of the ICON, the data acquired from Verem, Tuticorin, and Mandapam stations and the comparison method used.

3.1 Integrated Coastal Observation Network

The in-house designed and developed Internet-accessible real-/near-real-time reporting cellular-based sea level, sea state, and surface meteorological (Met) stations deployed at several locations

on the Indian coasts and islands is described in detail by Prabhudesai.¹⁹ The network of autonomous weather stations (AWS), sea-level gauges, and wave rider buoys as shown in Fig. 3 are incorporated in the ICON. The sea-level and surface meteorological data are acquired using dedicated Linux-based data loggers and uploaded to an Internet server at 5- and 10-min intervals, respectively, with the use of GPRS cellular modems. The sensors and data loggers are powered from sealed lead acid batteries, which are charged through solar panels (Figs. 2 and 3). The ICON provides graphical presentation of sea-level information [observed sea level, predicted tide, sea-level residual (SLR)] and surface meteorological information (such as vector-averaged wind speed and direction, barometric pressure, atmospheric temperature, relative humidity, solar radiation, and rainfall). The network maintains accurate time-stamp of the dataset through Internet-time synchronization using network time protocol. The ICON provides several benefits, such as remote monitoring of individual stations, remote health monitoring to aid timely maintenance, and periodic arrival of data streams from all stations at a single central server. The ICON data could be assimilated to real-time running of numerical models for operational forecast. The NIO network allows Internet-based real-/near-real-time tracking and monitoring of sea level, sea state, and meteorological conditions along the Indian coasts and islands and from almost anywhere having cellular connectivity. This is of considerable practical significance during natural disasters such as storms, storm surges and tsunamis.

3.2 Data

Sea-level data are collected off Goa [Fig. 1(b)] using real-time reporting pressure and radar gauges at Verem, located near the mouth of the Mandovi estuary, from January 2009 to May 2010. The sea-level gauge instruments are described in detail by Prabhudesai et al.²⁰ The PG data are sampled at 2 Hz frequency for 5-min durations (600 samples), averaged, and subsequently recorded in the data-logger at every 5 min. The RG samples are acquired over a 30-s window at 1-min intervals and averaged over 5-min intervals. Atmospheric pressure measurements collected from an AWS installed ~5 km away from the sea-level station are used for retrieving sea-level measurements from the absolute pressure (i.e., water pressure + atmospheric pressure) measurements acquired by the subsurface PG. For comparison, we have used time-series data at 10-min intervals. The recording-type PGs deployed at Tuticorin and Mandapam acquired data at an interval of 10 min with an integration duration of 1 min. The AWS was installed at Mandapam near the RG (~500 m) and is ~115 km from Tuticorin. The barometric pressure from this AWS is used for atmospheric pressure correction for both the PGs at Tuticorin and Mandapam, as the atmospheric perturbations have spatial characteristic of a few hundred kilometers (Table 2).

3.3 Comparison Method

To evaluate the accuracy or compare different measurement systems, the difference or error, especially the root-mean-square error (RMSE), is used as the parameter. As discussed by Willmott et al.,^{21,22} correlation coefficient (r) and its square, the coefficient of determination (r^2), may not be consistently related to the accuracy of predictions. Therefore, we compute and report the summary measures such as mean, standard deviation, the intercept, and slope of the least square regression with PG on y -axis and RG on x -axis. The different measures

Table 2 Summary of observations. The data used for analysis are at every 10-min interval and the time is in IST.

Station	Location	Distance between RG and PG	Measurement duration
Verem	15.5019° N 73.8121° E	50 m	January 1, 2009 to May 31, 2010
Tuticorin	08.7499° N 78.2022° E	500 m	June 21, 2010 to March 14, 2011
Mandapam	09.2713° N 79.1321° E	10 m	June 19, 2010 to March 12, 2011

are derived from the fundamental quantity $(P_i - O_i)$, where P is predicted measurements under test and O is the reference standard. In the present study, the measurements from RG (PG) refer to $O(P)$. The types of difference measures calculated are briefly defined below (for detailed explanation, please refer to Willmott).²³

$$\text{Mean absolute error (MAE)} = N^{-1} \sum_{i=1}^N |P_i - O_i|. \quad (2)$$

$$\text{RMSE} = \left[N^{-1} \sum_{i=1}^N (P_i - O_i)^2 \right]^{0.5}. \quad (3)$$

The systematic portion of the error is written as

$$\text{RMSE}_s = \left[N^{-1} \sum_{i=1}^N (\hat{P}_i - O_i)^2 \right]^{0.5}, \quad (4)$$

while the unsystematic part is

$$\text{RMSE}_u = \left[N^{-1} \sum_{i=1}^N (P_i - \hat{P}_i)^2 \right]^{0.5}. \quad (5)$$

The index of agreement (d) is of the form

$$d = 1 - \left[\frac{\sum_{i=1}^N (P_i - O_i)^2}{\sum_{i=1}^N (|P'_i| + |O'_i|)^2} \right], \quad 0 \leq d \leq 1, \quad (6)$$

where N is the number of data points, $\hat{P}_i = a + bO_i$ is the least square regression with the intercept (a) and slope (b), $P'_i = P_i - \bar{O}$ and $O'_i = O_i - \bar{O}$.

4 Results

Sea-level measurements reported by radar and pressure gauges during January 2009 to May 2010 from Verem, Goa, are shown in Fig. 4. Both the systems reported a tidal range up to 250 cm with fortnightly variation in spring and neap tides [Fig. 4(a) and 4(b)]. The tides off Verem have a “form number” of 0.64, implying that the tides are mixed, mainly of semi-diurnal nature.²⁴ When the tidal signal was removed from the sea-level records using the TASK²⁵ tidal analysis and prediction algorithm, both the systems produced similar SLRs, as shown in Fig. 4(c) and 4(d). The monthly variability is presented in Fig. 5 with negligible difference. The high residual variability ($\sim 163 \text{ cm}^2$) seen in November 2009 is the response of the sea level to the tropical cyclonic storm Phyan, which developed in winter in the southeastern Arabian Sea and swept northward along the eastern Arabian Sea during November 9 to 12, 2009.²⁶ However, the tidal range at Tuticorin (Mandapam) during the measurement period (Table 1) is $\sim 125(126)$ cm [Fig. 6(a), 6(b), 6(d), and 6(e)]. The tides are amplified as they propagate from south to north due to topological/bathymetric variation [Fig. 1(a)]. The mean absolute difference at Tuticorin (Mandapam) is $\sim 2.1(1.1)$ cm, as shown in Fig. 6(c) and 6(f) (Table 3).

To evaluate and compare the RGs and PGs, the anomaly (i.e., mean value of the time series) has been removed: scatter plots along with quantitative indices are shown in Fig. 7 (also refer to Table 3). From Fig. 7(a) to 7(c), it is clear that for all the three sites, the slope (b) is 1 and bias (a) is less than 0.6 cm. Also, it appears that the variability of sea level is higher at Tuticorin than Mandapam, with an energy of ~ 7.48 and 2.15 cm^2 , respectively (Table 4), which may be due to the focusing effect of waves near the southern tip of India. Figure 7(d) to 7(f) show the percentage occurrence of differences at the three sites, respectively. Examination of the summary position and scale parameters (Table 3) of RGs [i.e., mean of RG ($\bar{R}\bar{G}$) and standard deviation (S_{Rg})] compares well with the corresponding PGs (i.e., $\bar{P}\bar{G}$, S_{Pg}). The regression parameters

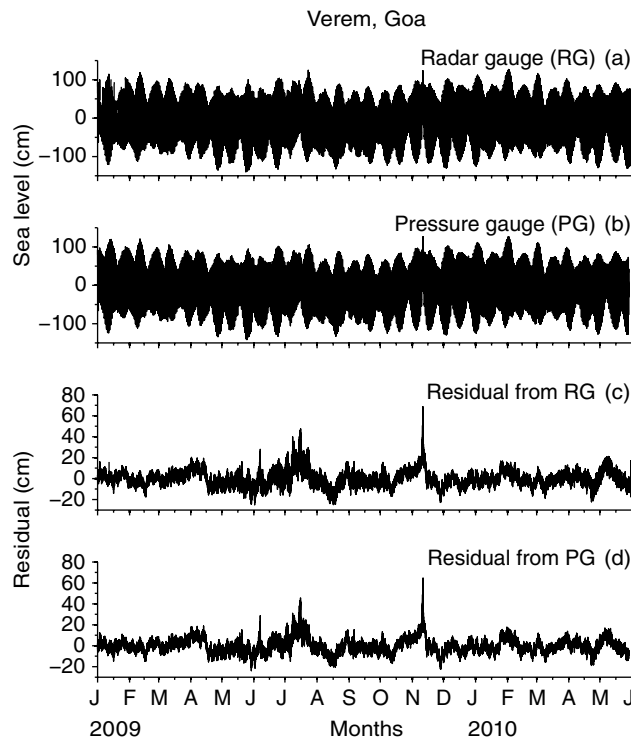


Fig. 4 Sea-level measurements at Goa using (a) RG, (b) PG, and respective residuals from (c) RG and (d) PG.

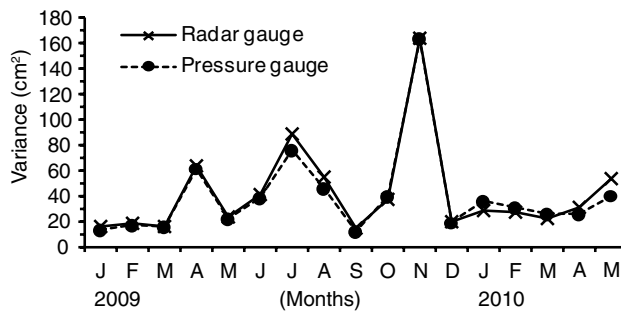


Fig. 5 Seasonal sea-level residual variability at Verem, Goa.

(a and b) show similar linear observations. MAE at Verem and Tuticorin is ~ 2 cm; however, at Mandapam it is less (~ 1.1 cm). RMSE, which results from the square of $(P_i - O_i)$, tends to inflate when the extreme values are present. RMSE, therefore, can generally be regarded as a high estimate of MAE. RMSE at Verem and Tuticorin is ~ 2.7 cm and at Mandapam it is ~ 1.5 cm. $RMSE_s$ is systematic linear function of differences, and it is ~ 0.6 cm at Verem and ~ 0.01 cm at Tuticorin and Manadapam, respectively. With the appropriate parameterization of the model, $RMSE_s$ can be substantially reduced, and therefore $RMSE_u$ can be interpreted as a potential measure of accuracy.²³ The index of agreement (d) and the coefficient of correlation (r) at significance level (95%) is same (0.99) at all the locations. The indices discussed above are listed in Table 3, and they provide a brief evaluation and comparison of PGs and RGs at Verem, Tuticorin, and Mandapam.

We have also estimated tidal constituents from the RG and PG data at Verem, Goa, using harmonic analysis. The basis of harmonic analysis is the assumption that the tidal variations can be represented by a finite number n , harmonic terms of the form²⁷

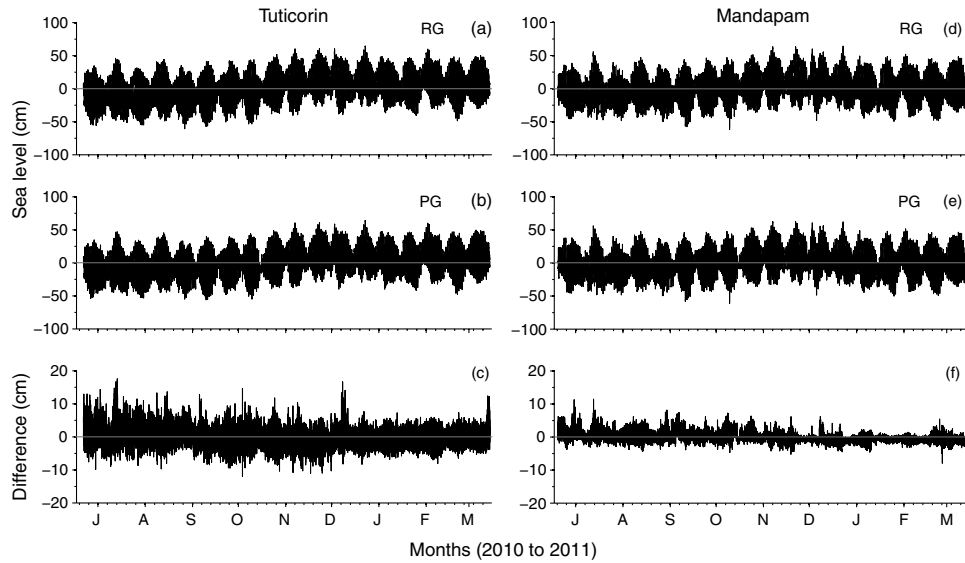


Fig. 6 Sea-level measurements at Tuticorin using (a) RG, (b) PG, and (c) difference (PG–RG), and at Mandapam using (d) RG, (e) PG, and (f) difference (PG–RG).

Table 3 Quantitative measures of comparison between RG and PG at different coastal locations of India. The terms N , a , b , d , and r are dimensionless, while the remaining terms have the units in cm.

Location	\bar{R}_G	\bar{P}_G	s_{rg}	s_{pg}	N	a	b	MAE	RMSE	RMSE _s	RMSE _u	d	r
Verem	0.00	0.00	48.72	48.53	72,788	1	+0.56	1.91	2.69	0.56	2.86	0.99	0.99
Tuticorin	0.00	0.00	20.92	20.58	38,082	1	+0.01	2.11	2.73	0.01	2.73	0.99	0.99
Mandapam	0.00	0.00	20.14	19.99	37,929	1	-0.01	1.11	1.46	0.01	1.47	0.99	0.99

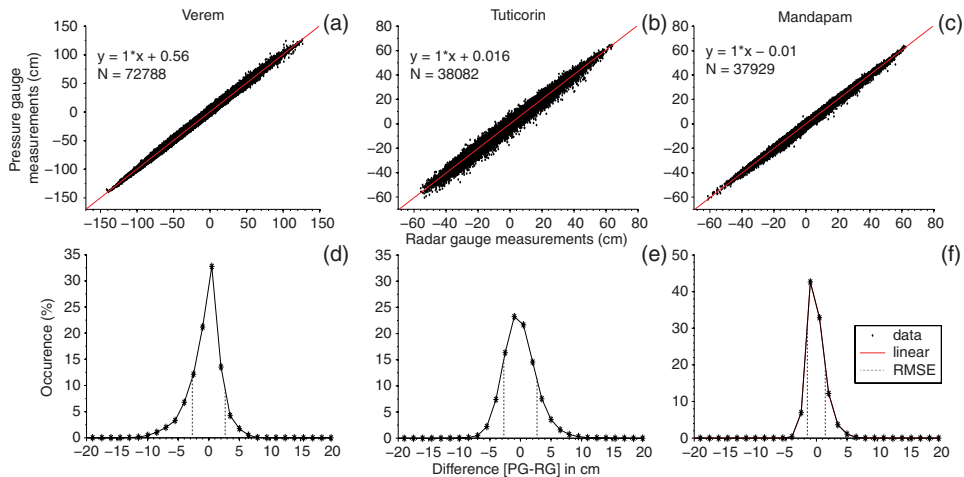


Fig. 7 Scatter plots of sea-level measurements using RG versus PG along with linear fit shown as red line at (a) Verem, (b) Tuticorin, and (c) Mandapam. The percentage occurrence of the difference (PG–RG) along with respective RMSEs are marked with dashed lines at (d) Verem, (e) Tuticorin, and (f) Mandapam. N is number of data points at respective station.

Table 4 Statistical inferences from the difference between PG and RG measurements of sea level.

Station	Verem		Tuticorin		Mandapam	
	d_0	d_1	d_0	d_1	d_0	d_1
Variance (cm ²)	16.11	6.95	10.46	7.48	6.42	2.15
RMSE (cm)	4.02	2.69	3.24	2.73	2.55	1.46

$$H_n \cos(\sigma_n t - g_n), \tag{7}$$

where H_n is an amplitude (cm), g_n is a phase lag (deg) on the equilibrium tide at Greenwich (local position in the present study), σ_n is an angular speed (degree per mean solar hour). Table 5 shows the main tidal constituents along with their description, time period (days), amplitudes (cm), and phase (deg) determined from the radar and pressure gauges during the study duration (see Fig. 8). The main diurnal and semi-diurnal tidal constituents are within ± 2 mm in magnitude and within 1.5 deg in phase. However, the exception is the annual (Sa) and semi-annual (Ssa), for which the amplitudes (phases) differ by 10.7 (−3.2 deg) and 2.2 mm (11.8 deg), respectively. This could reflect, to some extent, the seasonal changes in the density of the water in the Mandovi estuary, from which measurements were collected, and could also be due to the limited data series of ~ 1 year duration.

Table 5 Major tidal constituents obtained from RG and PG deployed at Verem, Goa, during January 2009 to May 2010. For the details of harmonic tidal constituents, please refer to Pugh.²⁷

Tidal constituents	Time period (d)	Description of tidal constituents	Magnitude (cm)		Difference (mm)	Phase (deg)		Difference (deg)
			RG	PG		RG	PG	
S_a	365.2	Solar annual	6.65	7.72	−10.7	312.96	316.15	−3.2
S_{sa}	182.6	Solar semi-annual	3.71	3.49	2.2	216.37	204.60	11.8
M_m	27.55	Lunar monthly	2.06	1.68	3.8	347.24	345.86	1.4
M_{sf}	14.77	Variational fortnightly	1.33	1.15	1.8	38.08	31.38	6.7
M_f	13.66	Lunar fortnightly	1.27	1.31	−0.4	53.11	51.64	1.5
Q_1	1.12	Larger elliptical lunar	3.02	2.98	0.4	52.77	53.02	−0.2
O_1	1.076	Principal lunar	14.82	14.75	0.7	55.52	55.56	0.0
P_1	1.003	Principal solar	8.40	8.49	−0.9	56.48	56.14	0.3
K_1	0.997	Luni-solar declinational diurnal	30.00	30.09	−0.9	58.72	58.94	−0.2
J_1	0.962	Elliptical lunar	1.71	1.71	0.0	71.07	71.78	−0.7
N_2	0.527	Larger elliptical lunar	12.14	12.20	−0.6	297.73	298.17	−0.4
ν_2	0.526	Larger evectional	2.41	2.34	0.6	301.75	302.80	−1.0
M_2	0.518	Principal lunar	51.94	51.77	1.7	320.08	320.43	−0.3
L_2	0.508	Smaller elliptical lunar	1.48	1.40	0.8	343.55	343.42	0.1
S_2	0.5	Principal solar	18.37	18.22	1.4	358.25	358.86	−0.6
K_2	0.499	Luni-solar declinational	4.74	4.74	0.0	352.60	353.67	−1.1

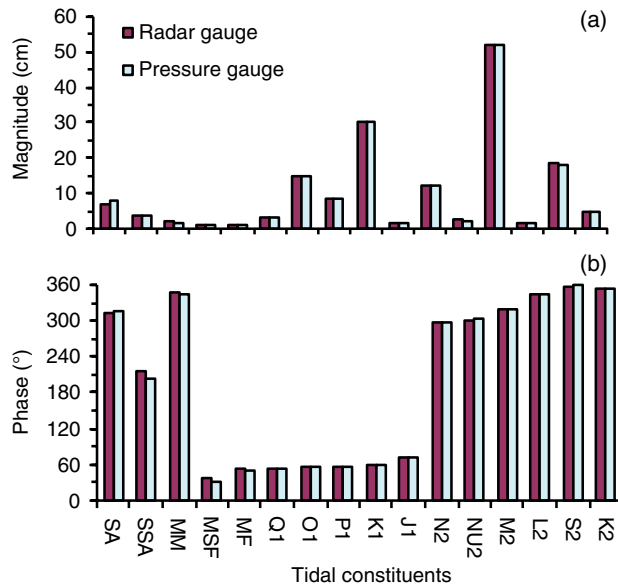


Fig. 8 Major tidal constituents at Verem, Goa, obtained using RG and PG. (a) Amplitude and (b) phase.

Atmospheric pressure variations measured by the AWS at Dona Paula, Goa, are presented in Fig. 9(a). The atmospheric pressure anomaly shows annual cycle, where the atmospheric pressure is low (high) during June to July (January). The atmospheric pressure variations are within ± 10 mb. The sea-level measurements obtained from the subsurface PG may lead to over- or underestimates, if atmospheric pressure corrections are not applied (inverse barometric effect ~ -1 cm/mbar). The sea level is first estimated from the PG without using measured atmospheric pressure, and instead, standard values such as $p_a = 1004.5$ mb, $\rho = 1.020$ g cm $^{-3}$, and $g = 980.665$ cm s $^{-2}$ were used [Eq. (1)]. Thus d_0 is the difference between the sea-level measurements obtained from PG and RG, where a constant value of barometric pressure is used in

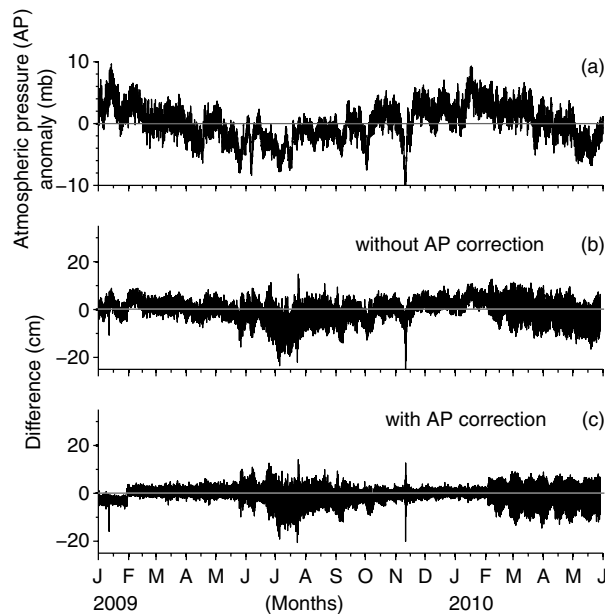


Fig. 9 Time series of (a) atmospheric pressure (AP) anomaly (mb), (b) difference (d_0) between sea level estimated from pressure and radar gauge without measured atmospheric pressure correction, and (c) difference (d_1) between sea level estimated using PG and RG with measured atmospheric pressure correction.

estimating the sea level from PG [Fig. 9(b)]. This situation may arise when the sea-level measurements are made using pressure sensors at remote/offshore locations, where atmospheric pressure measurements are not available. With reference to Fig. 9(c), d_1 is the difference between the sea-level measurements obtained from PG and RG, wherein the measured barometric pressure is used in estimating the sea level from PG. The availability of atmospheric pressure data provides an excellent opportunity to estimate its effect on sea-level measurements obtained using PGs.

Table 4 presents the improvement in RMSEs at three study sites, when PG measurements are included with simultaneous barometric corrections. The difference (d_0) at Verem is shown in Fig. 9(b), with a variance of $\sim 16.1 \text{ cm}^2$. The difference (d_1) between PG and RG with measured atmospheric pressure correction [Eq. (1)] is shown in Fig. 9(c). The variance in the difference reduces to $\sim 7.0 \text{ cm}^2$. The RMSE for the difference with (d_1) and without (d_0) atmospheric pressure corrections is estimated to be 2.6 and 4.0 cm, respectively, as listed in Table 4. Similarly, the variation in d_0 at Tuticorin (Mandapam) is $10.46 (6.42) \text{ cm}^2$, which reduced to $7.48 (2.15) \text{ cm}^2$ for d_1 .

5 Summary and Conclusions

The development of ICON consisting of sea-level gauges and AWS was initiated in the year 2005, immediately after the occurrence of December 2004 Sumatra tsunami, and the first real-/near-real-time reporting sea-level gauge based on pressure sensor was installed at Verem, Goa, in September 2005. However, presently all our sea-level stations use radar sensor, except at Verem, Goa, where both real-/near-real-time sea-level gauges based on radar and pressure sensors are in operation. This also meets the GLOSS recommendations to keep an overlapping period of at least 1 year to assess the reliability and accuracy of new equipment²⁸ with enough data to make a comparison between the old and the new technology. In fact, the “perfect” sea-level gauge does not exist, and various technologies/options need to be evaluated for different applications. For example, PGs will be more suitable for deployment in offshore locations where height of the RG tower is a limitation and where there are jetties with high fishing activity.

This study describes a comparison of sea-level measurements from downward-looking aerial microwave radar and absolute subsurface PGs from Verem (Goa) and Tuticorin and Mandapam (Tamil Nadu), India. As recommended by Willmott,²³ the comparisons of RG and PG are based on the difference measures and supported by graphical plots, RMSE, as well as systematic and unsystematic proportions or magnitudes. The results thus obtained suggest that both the systems function very well and produce similar tidal constituents. The sea-level measurements from subsurface PG with measured barometric pressure correction applied at Verem, Tuticorin, and Mandapam indicate an improvement in RMSE by 33%, 15%, and 42%, respectively, in the present study. However, during rainy season, the PG may underestimate the sea-level measurements due to water density variations resulting from fresh water influx from the river. For example, in a similar study at Verem from September 2007 to March 2009, Mehra et al.²⁹ reported the variance of difference between the radar and absolute PG as 15.9 cm^2 , which reduced to 5.7 and 4.0 cm^2 , respectively, when atmospheric pressure alone and atmospheric pressure together with water density variations were introduced for obtaining sea level from an absolute PG. Also, Joseph et al.³⁰ reported in a study at Marmugao Port, Goa, from June 1995 to July 1998 that the surface water density varied between 1.020 and 0.996 g cm^{-3} . During June to July 2008 at Verem sea-level gauge, which is located in the Mandovi estuary, the water density remained low ($\sim 1.000 \pm 0.005 \text{ g cm}^{-3}$), and by September it increased to $\sim 1.020 \text{ g cm}^{-3}$, remained at this level until May, and then sharply declined to $1.000 \pm 0.005 \text{ g cm}^{-3}$ by June.²⁹ The water density measurement site is $\sim 2.4 \text{ km}$ upstream from the PG location in the Mandovi estuary. The effective density used at Verem, Goa, is 1.020 g cm^{-3} , $g = 980.665 \text{ cms}^{-2}$, and atmospheric pressure is obtained from AWS. However, the variations in the effective density $\nabla\rho = (1.020 - 0.995) = 0.025 \text{ g cm}^{-3}$ could lead to an underestimation of 2.45% in sea level by the PG. The long-term measurement of water density is practically difficult, but the importance of concurrent measurements of atmospheric pressure along with the PG measurements is duly emphasized in the present study.

It is worth mentioning that the sea-level station deployed for the present study measures the sea level in a completely different way than the traditional float or bubbler gauges. The ICON is developed with simple supporting structure to mount the sensors, powered by solar energy, and communicating data (using cellular modems) automatically to a base server located at CSIR-NIO, Goa. The system does not need expensive infrastructure, such as stilling-well, intake pipes, or cabins, normally seen in ports. However, these features could present some drawback, if the sites are exposed to harsh environment and lack security. With prior survey of the sites, the drawback of harsh environments and security aspects are minimized and we, therefore, have been able to operate the network of such stations (see <http://inet.nio.org/>) successfully since September 2005. The sea-level gauges at Verem and Kavaratti Island enabled real-time monitoring of the tsunami at Goa and Kavaratti Island due to the M_w 8.4 earthquake in Sumatra on September 12, 2007.³¹ In particular, sea-level gauges, surface meteorological instruments, and wave-rider buoys in the network enabled real-time monitoring of the response of west India coastal waters and Kavaratti lagoon to the November 2009 tropical cyclone Phyan.²⁶ It is expected that relatively inexpensive and simple networks, similar to the one described in this paper, will be affordable to economically moderate institutions in their natural hazard mitigation efforts.

Acknowledgments

The authors acknowledge the support of the Naval Office Verem, Goa, for providing a safe and secure site. The authors thank Mr. A. Shirgoankar for his consistent support in keeping the systems operational. The authors also acknowledge Director CSIR-NIO, Goa, and CSIR, New Delhi, for all the support and encouragement. This is CSIR-NIO contribution No. 5358.

References

1. J. A. Church et al., "Changes in sea level," in *Climate Change: The Scientific Basis*, J. T. Houghton et al., Eds, pp. 639–693, Cambridge University Press, London (2001).
2. A. Cazenave and R. S. Nerem, "Present-day sea level change: observations and causes," *Rev. Geophys.* **42**(3), 1–20 (2004), <http://dx.doi.org/10.1029/2003RG000139>.
3. S. M. Griffies and R. J. Greatbatch, "Physical processes that impact the evolution of global mean sea level in ocean climate models," *Ocean Model.* **51**, 37–72 (2012), <http://dx.doi.org/10.1016/j.ocemod.2012.04.003>.
4. T. Chang-Kou and W. Carl, "Sampling errors of the global mean sea level derived from TOPEX/Poseidon altimetry," *Acta Oceanol. Sin.* **30**(6), 12–18 (2011), <http://dx.doi.org/10.1007/s13131-011-0156-x>.
5. D. R. Richard and D. A. Byrne, "Bottom pressure tides along a line in the southeast Atlantic Ocean and comparisons with satellite altimetry," *Ocean Dynam.* **60**(5), 1167–1176 (2010), <http://dx.doi.org/10.1007/s10236-010-0316-0>.
6. D. P. Chambers, M. A. Merrifield, and R. S. Nerem, "Is there a 60-year oscillation in global mean sea level?," *GRL* **39**(18), L18607 (2012), <http://dx.doi.org/10.1029/2012GL052885>.
7. P. L. Woodworth et al., "Evidence for the accelerations of sea level on multi-decade and century timescales," *Int. J. Climatol.* **29**(6), 777–789 (2009), <http://dx.doi.org/10.1002/joc.1771>.
8. M. Feng, Y. Li, and G. Meyers, "Multidecadal variations of Fremantle sea level: footprint of climate variability in the tropical Pacific," *Geophys. Res. Lett.* **31**(16), L16302 (2004), <http://dx.doi.org/10.1029/2004GL019947>.
9. L. Bernstein et al., "Synthesis report: climate change 2007," in *An Assessment of the Intergovernmental Panel on Climate Change* adopted section by section at IPCC Plenary XXVII, Valencia, Spain (November 12–17 2007).
10. V. Titov et al., "The global reach of the 26 December 2004 Sumatra tsunami," *Science* **309**(5743), 2045–2048 (2005), <http://dx.doi.org/10.1126/science.1114576>.

11. A. Joseph et al., "The 26 December 2004 Sumatra tsunami recorded on the coast of West Africa," *African J. Marine Sci.* **28**(3&4), 705–712 (2006), <http://dx.doi.org/10.2989/18142320609504219>.
12. A. Joseph and R. G. Prabhudesai, "Need of a disaster alert system for India through a network of real time monitoring of sea level and other meteorological events," *Curr. Sci.* **89**(5), 864–869 (2005).
13. A. Joseph, *Tsunamis: Detection, Monitoring, and Early-Warning Technologies*, Elsevier Science & Technology, Burlington, Massachusetts (2011).
14. M. B. Martin, B. P. Gomez, and A. E. Fanjul, "The ESEAS-RI sea level test station: reliability and accuracy of different tide gauges," *Int. Hydrographic Rev.* **6**(1), 44–53 (2005).
15. M. B. Martin, R. Le Roy, and G. Woppelmann, "The use of radar tide gauges to measure variations in sea level along the French coast," *J. Coastal Res.* **24**(4A), 61–68 (2008), <http://dx.doi.org/10.2112/06-0787.1>.
16. S. Kranz, T. Zenz, and U. Barjenbruch, "Radar: is it a new technology applicable to water level gauging?," *Phys. Chem. Earth (C)* **26**(10–12), 751–754 (2001), [http://dx.doi.org/10.1016/S1464-1917\(01\)95020-2](http://dx.doi.org/10.1016/S1464-1917(01)95020-2).
17. P. L. Woodworth and D. E. Smith, "A one year comparison of radar and bubbler tide gauges at Liverpool," *Int. Hydrographic Rev.* **4**(3), 2–9 (2003).
18. Intergovernmental Oceanographic Commission, "Manual on sea level measurement and interpretation, Vol. 4: an update to 2006," p. 78, Intergovernmental Oceanographic Commission of UNESCO, Paris (IOC Manuals and Guides No.14, vol. IV; JCOMM Technical Report No.31; WMO/TD. No. 1339) (English) (2006).
19. R. G. Prabhudesai et al., "Integrated Coastal Observation Network (ICON) for real-time monitoring of sea-level, sea-state, and surface-meteorological data," presented at *Proc. Oceans'10 MTS/IEEE*, pp. 20–23, Seattle, Washington (September 2010).
20. R. G. Prabhudesai et al., "Development and implementation of cellular-based real-time reporting and Internet accessible coastal sea level gauge: a vital tool for monitoring storm surge and tsunamis," *Curr. Sci.* **90**(10), 1413–1418 (2006).
21. C. J. Willmott, "On the validation of models," *Phys. Geogr.* **2**(2), 184–194 (1981).
22. C. J. Willmott et al., "Statistics for the evaluation and comparison of models," *JGR* **90**(C5), 8995–9005 (1985), <http://dx.doi.org/10.1029/JC090iC05p08995>.
23. C. J. Willmott, "Some comments on the evaluation of model performance," *Bull. Am. Meteorol. Soc.* **63**(11), 1309–1313 (1982), [http://dx.doi.org/10.1175/1520-0477\(1982\)063<1309:SCOTEO>2.0.CO;2](http://dx.doi.org/10.1175/1520-0477(1982)063<1309:SCOTEO>2.0.CO;2).
24. T. S. Murty and R. F. Henry, "Tides in the Bay of Bengal," *J. Geophys. Res.* **88**(C10), 6069–6076 (1983), <http://dx.doi.org/10.1029/JC088iC10p06069>.
25. C. Bell, J. M. Vassie, and P. L. Woodworth, Tidal Analysis Software Kit 2000 (TASK-2000), POL/PSMSL Permanent Service for Mean Sea Level, Proudman Oceanographic Laboratory, United Kingdom (2000).
26. A. Joseph et al., "Response of west Indian coastal regions and Kavaratti lagoon to the November-2009 tropical cyclone Phyan," *Nat. Hazards* **57**(2), 293–312 (2011), <http://dx.doi.org/10.1007/s11069-010-9613-7>.
27. D. T. Pugh, *Tides, Surges and Mean Sea-Level*, John Wiley and Sons Ltd., New York (1987).
28. Intergovernmental Oceanographic Commission., "Manual on sea-level measurement and interpretation, Vol. 2: emerging technologies," Technical Series No. 14, Intergovernmental Oceanographic Commission, Paris (1994).
29. P. Mehra et al., "A one year comparison of radar and pressure tide gauge at Goa, west coast of India," in *Proc. Int. Symp. on Ocean Electronics*, P. R. S. Pillai and M. H. Supriya, Eds., pp. 173–183, IEEE, Cochin, India (2009).
30. A. Joseph et al., "Over-estimation of sea level measurements from water density anomalies within tide-wells: a case study at Zuari estuary, Goa," *J. Coastal Res.* **18**(2), 362–371 (2002).
31. R. G. Prabhudesai et al., "Cellular-based and Internet-enabled real-time reporting of the tsunami at Goa and Kavaratti Island due to Mw 8.4 earthquake in Sumatra on 12 September 2007," *Curr. Sci.* **94**(9), 1151–1157 (2008).



Prakash Mehra is principal scientist at CSIR—National Institute of Oceanography, Goa, India. He received his BTech degree in electronics and communication from Regional Engg. College of Calicut and MTech from Indian Institute of Technology, Chennai. He actively works and conducts research in the areas of sea-level and surface meteorological measurements and response of coastal sea-level to meteorological and tsunamigenic events. He has to his credit 16 peer-reviewed publications and two USA patents. He is a faculty member at the Indian Academy of Scientific and Innovative Research (AcSIR-School of Oceanography), wherein he teaches the technologies of sea-level and surface meteorological measurements. He has actively contributed to the establishment of a network of cellular-based and Internet-accessible real/near-real time sea-level and surface meteorological stations on the Indian coastlines and islands



Ramachandra Gopal Prabhu Desai joined National Institute of Oceanography Goa in the year 1979. He has worked on the design and development of instrumentation for measurement of sea level, surface meteorological parameters and has contributed to development of several other systems developed at NIO. His interests include marine instrumentation and embedded systems. He has been responsible for design and development of Integrated Coastal Observation System at NIO, Goa. He has several publications related to his research interests to his credit.



Antony Joseph who was formerly chief scientist at CSIR—National Institute of Oceanography in India, conducted research in the areas of sea-level and surface meteorological measurements. He is the sole author of two Elsevier (New York) books titled “Tsunamis: Detection, Monitoring, and Early-Warning Technologies,” published in February 2011, and “Measuring Ocean Currents: Tools, Technologies, and Data,” scheduled to be published in October 2013. He was a faculty member at the Indian Academy of Scientific and Innovative Research (AcSIR-School of Oceanography), wherein he taught the technologies of sea-level and oceanic current measurements. Presently he is World Bank’s technical expert to advise and supervise establishment of permanent sea level stations at the Indian Part of Sunderbans for long-term collection of sea level data for climate related studies. He led the establishment of an in-house-designed sea-level station in Ghana (West Africa) for IOC-UNESCO and provided high-quality data on the arrival of the December 2004 Sumatra tsunami at the central east Atlantic coast, thereby contributing to the understanding of the global extent of this tsunami. Subsequent to the December 2004 Indian Ocean tsunami, he and a team of colleagues contributed immensely to the establishment of a cost-effective network of cellular-based and Internet-accessible real/near-real time reporting sea-level, sea-state and surface meteorological stations on the Indian coastlines and islands



Vijay Kumar received his BE degree in electronics and telecommunication from Shivaji University, Kolhapur and MSc (Engg.) degree in atmosphere and ocean science from Indian Institute of Science, Bangalore, India, in 2008 and 2010 respectively. He has to his credit seven international and four national patents, and publications in marine instrumentation. He has been involved in design and development of sea level gauges and autonomous weather stations, setup of Internet-accessible near-real time network of sea levels and meteorological stations along the Indian coast. Currently, he is working on development of air-sea flux observation system from research vessel.



Yogesh Agarvadekar completed his diploma in electronics engineering from Govt. Polytechnic, Panaji, Goa in the year 2002 and presently working as technical assistant at CSIR—National Institute of Oceanography, Goa, India. He has been involved in the development and establishment of Integrated Coastal Observation Network (ICON) of sea-level gauges and autonomous weather stations (AWS) along the coast of India. He has also modified AWS for research vessels. He is team member of NIOs mooring group, which operates shallow and deep sea moorings with ADCP, RCM, temperature recorder, sediment traps along Indian coast. His core interest is in testing of electronics, development of software for microcontrollers, Linux-embedded systems and server-side applications for collecting, storing and display of real-time data from different stations.



Ryan Luis is working as technical assistant at CSIR—National Institute of Oceanography, Goa, India. He completed his diploma in electronic engineering from Agnel Polytechnic Verna-Goa. He has been involved in fabrication, evaluation and operation of autonomous weather station (AWS) and sea-level gauges at various remote locations of India coast. He has also participated in various oceanographic cruises, wherein he has been involved in operation and deployment of CTD, moorings with ADCP, current meter, and sediment trap.



Lalsab Nadaf was working at CSIR—National Institute of Oceanography (NIO), Goa, India, as project assistant from August 2010 to 31 July, 2012. He completed his MSc in electronics from Goa University in 2010. At CSIR-NIO, he has been responsible for testing and evaluation of sensors, installation and uninterrupted operation of the indigenously developed instruments like autonomous weather station (AWS), tide gauges (radar and pressure based), along the various remote coastal locations of India. He had been actively involved in the analysis of sea-level and surface meteorological data for scientific documentation